Insulin Receptor Isoform A, a Newly Recognized, High-Affinity Insulin-Like Growth Factor II Receptor in Fetal and Cancer Cells

F. FRASCA,[1] G. PANDINI,[1] P. SCALIA,[1] L. SCIACCA,[1] R. MINEO,[1] A. COSTANTINO,[1]
I. D. GOLDFINE,[2] A. BELFIORE,[3] AND R. VIGNERI[1]*

*Istituto di Medicina Interna, Malattie Endocrine e del Metabolismo, University of Catania, Ospedale Garibaldi,
95123 Catania,[1] and Cattedra di Endocrinologia, University of Catanzaro, Policlinico Mater Domini,
Catanzaro,[3] Italy, and Division of Diabetes and Endocrine Research,
University of California, San Francisco, California 94115[2]*

Insulin-like growth factor II (IGF-II) is a peptide growth factor that is homologous to both insulin-like growth factor I (IGF-I) and insulin and plays an important role in embryonic development and carcinogenesis. IGF-II is believed to mediate its cellular signaling via the transmembrane tyrosine kinase type 1 insulin-like growth factor receptor (IGF-I-R), which is also the receptor for IGF-I. Earlier studies with both cultured cells and transgenic mice, however, have suggested that in the embryo the insulin receptor (IR) may also be a receptor for IGF-II. In most cells and tissues, IR binds IGF-II with relatively low affinity. The IR is expressed in two isoforms (IR-A and IR-B) differing by 12 amino acids due to the alternative splicing of exon 11. In the present study we found that IR-A but not IR-B bound IGF-II with an affinity close to that of insulin. Moreover, IGF-II bound to IR-A with an affinity equal to that of IGF-II binding to the IGF-I-R. Activation of IR-A by insulin led primarily to metabolic effects, whereas activation of IR-A by IGF-II led primarily to mitogenic effects. These differences in the biological effects of IR-A when activated by either IGF-II or insulin were associated with differential recruitment and activation of intracellular substrates. IR-A was preferentially expressed in fetal cells such as fetal fibroblasts, muscle, liver and kidney and had a relatively increased proportion of isoform A. IR-A expression was also increased in several tumors including those of the breast and colon. These data indicate, therefore, that there are two receptors for IGF-II, both IGF-I-R and IR-A. Further, they suggest that interaction of IGF-II with IR-A may play a role both in fetal growth and cancer biology.

Insulin-like growth factors I and II (IGF-I and IGF-II) are related peptides with homology to the hormone insulin. In most cells, IGFs are major growth factors whereas insulin predominantly regulates glucose uptake and cellular metabolism. It is widely believed that IGF-I and IGF-II exert their effects through the type 1 IGF receptor (IGF-I-R), a transmembrane protein with high homology to the insulin receptor (IR) (55). IGF-II also binds to the mannose-6-phosphate receptor. This receptor is involved in the transport of lysosomal enzymes, is believed to act as a degradation pathway for IGF-II, and has no signaling activity for cell growth (58). However, there is evidence suggesting that under certain conditions, IGF-II may signal via the IR. First, dwarf transgenic animals with disruption of the IGF-II gene are born more severely growth retarded than are dwarf transgenic animals with disruption of the IGF-I-R gene, suggesting that IGF-II may activate another receptor (27). Genetic analysis of dwarfing phenotypes suggests that this receptor may be the IR (28). Second, in IGF-I-R-deficient mouse fibroblasts transfected with the human IR, IGF-II stimulates cell proliferation through the IR (34). However, since prior data have indicated that IGF-II binds to the IR with relatively low affinity (approximately 1% that of insulin) (45), the interaction of IGF-II with the IR remains to be clarified.

The human IR exists in two isoforms, isoform A (IR-A) and isoform B (IR-B). Alternative splicing of a small exon (exon

11) of the IR gene results in two transcripts, in which 36 additional nucleotides encoding 12 amino acids (residues 718 to 729) at the carboxyl terminus of the receptor α-subunit are either excluded (Ex11− or type A insulin receptor [IR-A]) or included (Ex11+ or type B insulin receptor [IR-B]) (33). The relative expression of the two isoforms varies in a tissue-specific manner. IR-A is expressed predominantly in central nervous system and hematopoietic cells, while IR-B is expressed predominantly in adipose tissue, liver, and muscle, the major target tissues for the metabolic effects of insulin (33, 35). Small functional differences in insulin binding and IR activation have been described for these two isoforms. IR-A has a slightly higher binding affinity and IR-B has a more efficient signaling activity as evaluated by its tyrosine kinase activity and phosphorylation of insulin receptor substrate 1 (IRS-1) (22). Therefore, the biological roles of the two IR isoforms are unknown.

In this study, we have investigated how IGF-II interacts with each individual isoform of the IR (IR-A and IR-B). We now report that IGF-II binds with high affinity to and activates IR-A but not IR-B. IR-A, when activated by IGF-II, elicits predominantly mitogenic rather than metabolic effects. We also report that the relative expression of IR-A is predominant in fetal tissues and some cancers. These findings indicate that IR-A is an IGF-II receptor which plays a role in fetal growth and cancer biology.

MATERIALS AND METHODS

Materials. The pNTK2 expression vectors containing the cDNA for either IR-A (Ex11−) or IR-B (Ex11+) were kindly provided by Axel Ullrich (Munich, Germany). The pECE expression vector containing the cDNA encoding the human IGF-I-R was a gift of Richard Roth (Stanford, Calif.).

* Corresponding author. Mailing address: Cattedra di Endocrinologia, Ospedale Garibaldi, 95123 Catania, Italy. Phone: 39-095-32 62 90. Fax: 39-095-715 80 72. E-mail: segmeint@mbox.unict.it.

Dulbecco's modified Eagle's medium (DMEM), fetal calf serum, glutamine, gentamicin, Lipofectamine, IGF-I, and IGF-II were obtained from Gibco Laboratories (Paisley, United Kingdom). N-Acetyl-D-glucosamine, bovine serum albumin ([BSA] radioimmunoassay grade), bacitracin, phenylmethylsulfonyl fluoride (PMSF), puromicin, and porcine insulin were obtained from Sigma Chemical Co. (St. Louis, Mo.). Protein A-Sepharose was obtained from Pharmacia (Uppsala, Sweden). TyrA14-^{125}I-labeled insulin (specific activity, 13.3 MBq/µg) was kindly provided by R. Navalesi (Pisa, Italy). ^{125}I-labeled IGF-I (specific activity, 11.8 MBq/µg) was obtained from Dupont NEN (Dreieich, Germany). The following antibodies were used: anti-IR MA-20 monoclonal antibody, which reacts with the α-subunit at an epitope close to the insulin binding site (12), and anti-IGF-I receptor αIR3 monoclonal antibody, which reacts with the α-subunit at residues 223 to 274 (52) (Oncogene Research, Cambridge, Mass.); anti-IRS-1 and anti-IRS-2 polyclonal antibodies and antiphosphotyrosine monoclonal antibody (UBI, Lake Placid, N.Y.); anti-Shc polyclonal antibody (Transduction Laboratories, Lexington, Ky.); and phosphospecific extracellular signal-related kinase (ERK) polyclonal antibody and anti-ERK polyclonal antibody (New England Biolabs, Beverly, Mass.).

Cell cultures and tissues. NIH 3T3 and CHO cells were obtained from the American Type Culture Collection, and R$^-$ mouse fibroblasts (mouse 3T3-like cells derived from animals with a targeted disruption of the IGF-I-R gene) were kindly provided by Renato Baserga (Philadelphia, Pa.). Human dermal fibroblasts were obtained from both fetuses at 16 to 18 weeks gestational age after spontaneous abortion and from adult healthy volunteers. All cell types were routinely grown in DMEM supplemented with 10% fetal bovine serum and 1% penicillin-streptomycin. cDNAs from normal fetal and adult tissues including liver, muscle, kidney, brain (multiple-choice cDNAs) were obtained from Ori-Gene Technologies, Inc. (Rockville, Md.). Tissue specimens from both normal and neoplastic lungs, breasts, and colons were obtained at surgery and immediately stored in liquid nitrogen until processed.

Transfection experiments. Cells grown in 35-mm plates until they were 60 to 70% confluent were transfected for 5 h at 37°C with the pNTK2 expression vector containing the cDNA for either IR-A (Ex11−) or IR-B (Ex11+) (7) or with the pECE expression vector containing the cDNA encoding the IGF-I-R (53, 55) by using the Lipofectamine reagent (Gibco/BRL). R$^-$ cells were also cotransfected with pPDV6+ plasmid, which contains the puromicin resistance gene. Transfected cells were then washed twice with phosphate-buffered saline (PBS; pH 7.4), and complete medium was added. At 48 h after transfection, the cells were divided among three 100-mm petri dishes and cultured in selective medium containing 2.5 µg of puromicin per ml. Cell clones expressing similar amounts of IR-A, IR-B, and IGF-I R (70 to 100 ng/100 µg of protein; approximately 3 × 10^5 to 5 × 10^5 receptors/cell as measured by specific enzyme-linked immunosorbent assays [ELISAs] [42]) were selected for subsequent studies.

Binding studies. Binding studies were performed with intact cells grown to approximately 80% of confluence and serum starved for 16 h. After two washes with PBS, the cells were incubated in binding buffer (DMEM without sodium bicarbonate but with 50 mM HEPES, 1% BSA, and 0.06 mg of bacitracin per ml) in the presence of increasing concentrations of unlabelled ligands and 10 pM ^{125}I-insulin. After a 16-h incubation at 4°C, the cells were washed twice with cold 10 mM Tris-buffered saline, and the cell-associated radioactivity was measured.

IR autophosphorylation and activation of intracellular substrates (IRS-1, IRS-2, Shc, ERK1, and ERK2) in response to either insulin or IGF-II. (i) Preparation of whole-cell detergent lysates. Confluent cells were washed twice with PBS (pH 7.4) and serum starved for 48 h. The cells were then treated with 10 nM insulin or IGF-II for various times as indicated in the figure legends. Ligand stimulation was terminated by two washes with ice-cold PBS (pH 7.4), removal of excess liquid by aspiration, and addition of ice-cold lysis buffer (150 mM NaCl, 1% Nonidet P-40, 0.5% deoxycholate, 0.1% sodium dodecyl sulfate [SDS], 50 mM Tris [pH 7.4], 10 mM sodium pyrophosphate, 100 mM NaF, 2 mM PMSF, 2 mM sodium vanadate, 1 µg of pepstatin per ml, 1 µg of aprotinin per ml, 1 µg of leupeptin per ml). After being scraped, the samples were rotated for 15 min at 4°C. Insoluble material was separated from soluble extract by microcentrifugation at 10,000 × g for 10 min at 4°C. The protein concentration was determined by the Bradford assay (Bio-Rad, Hercules, Calif.).

(ii) Immunoprecipitation. Cell lysates were incubated at 4°C under constant rotation for 2 h with either 5 µg of anti-IR monoclonal antibody (MA-20), 5 µg of anti-IRS-1 and anti-IRS-2 polyclonal antibodies, and 4 µg of anti-Shc polyclonal antibody and then incubated for 1 h with protein A-Sepharose. The immunoprecipitates were then eluted and subjected to SDS-polyacrylamide gel electrophoresis and immunoblotting as described below.

(iii) Immunoblot analysis. Whole-cell lysates or the specific immunoprecipitates were subjected to reducing SDS-polyacrylamide gel electrophoresis on either 7.5% acrylamide gels (IR, IRS-1, and IRS-2) or 10% acrylamide gels (ERK1, ERK2, and Shc). After electrophoresis, the resolved proteins were transferred to nitrocellulose membranes and subjected to immunoblot analysis with an antiphosphotyrosine monoclonal antibody. For ERK activation studies, the blots were probed with a phosphospecific ERK polyclonal antibody (New England Biolabs) (40) and, after being stripped (in 100 mM Tris-HCl [pH 6.7]–10% SDS–100 mM β-mercaptoethanol for 30 min at 50°C), reprobed with anti-ERK polyclonal antibody. All immunoblots were revealed by an enhanced chemiluminescence method (Amersham, Little Chalfont, United Kingdom), autoradiographed, and subjected to densitometric analysis.

(iv) ELISA of phosphorylated IR and IRSs. Studies of IR, IRS-1, and IRS-2 phosphorylation were also carried out by a specific ELISA (3, 4). Briefly, 100 µl of the cell lysates prepared as described above was immunocaptured in Maxisorp plates coated with either anti-IR, anti-IRS-1, or anti-IRS-2 antibodies (2 µg/ml in 50 mM sodium bicarbonate [pH 9.0]) overnight at 4°C. After the plates were washed, the captured phosphorylated proteins were incubated with an antiphosphotyrosine-biotin-conjugated antibody (0.3 µg/ml in 50 mM HEPES [pH 7.6]– 150 mM NaCl–0.05% Tween 20–1% BSA–2 mM sodium orthovanadate–1 mg of bacitracin per ml–1 mM PMSF) for 2 h at 22°C and then with peroxidase-conjugated streptavidin. The peroxidase activity was determined colorimetrically by adding 100 µl of 3,3′,5,5′-tetramethylbenzidine (TMB [Kirkegaard & Perry Laboratories, Gaithersburg, Md.]) at 0.4 mg/ml in 0.1 M citrate-phosphate buffer (pH 5.0) with 0.4 µl of 5% H$_2$O$_2$ per ml and measuring the absorbance at 451 nm.

(v) In vitro IR phosphorylation. IR kinase activity was also measured in solubilized receptors. Unstimulated cell monolayers were solubilized as described above, and IR was immunocaptured in Maxisorb plates coated with the anti-IR antibody MA-20. The immunopurified receptor was then stimulated with various concentrations of either insulin or IGFs in the presence of ATP (10 mM), MgCl$_2$ (10 mM), and MnCl$_2$ (2 mM). After the plates were washed, the phosphorylated proteins were incubated with an antiphosphotyrosine-biotin-conjugated antibody and the reaction was detected as described above.

PI3-kinase activity measurement. Cell lysates were immunoprecipitated with either antiphosphotyrosine or anti-IRS-1 and anti-IRS-2 antibodies. Phosphoinositide 3-kinase (PI3-kinase) activity was measured in the immunoprecipitates, as previously described (16). Briefly, the immunoprecipitates were washed twice in PBS (pH 7.4) containing 1% Nonidet P-40 and 1 mM dithiothreitol (DTT), twice in 100 mM Tris (pH 7.4) containing 500 mM LiCl$_2$ and 1 mM DTT, and twice with 10 mM Tris pH 7.4 containing 100 mM NaCl and 1 mM DTT and then incubated with 0.2 mg of phosphatidylinositol and [γ-^{33}P]ATP (40 µM, 10 µCi) for 5 min. The reaction was stopped by adding 4 N HCl and CHCl$_3$-methanol (1:1). Samples obtained from the organic phase were then separated by thin-layer chromatography on silica plates and subjected to autoradiography. Phosphatidylinositol phosphate (PIP) spots on silica plates were cut out, and radioactivity was measured in a β-counter.

IR measurement. Fresh tissue specimens collected at surgery, carefully dissected by a pathologist, and immediately frozen were stored in liquid nitrogen until processed. Tissues were solubilized for 60 min at 4°C with 50 mM HEPES buffer (pH 7.6) containing 1 mM PMSF and 1% Triton X-100. The solubilized material was then centrifuged at 10,000 × g, and the supernatant was frozen at −80°C until assayed. The protein content in the cellular extracts was measured by the Bradford assay (Bio-Rad, Hercules, Calif.). IRs were captured by incubating cell or tissue lysates in Maxisorp immunoplates (Nunc, Roskilde, Denmark) precoated with 2 µg of MA-20 per ml. After the plates were washed, the immunocaptured receptors were incubated with the biotinylated anti-IR αCT-1 antibody (which recognizes a different epitope from MA-20) at 0.3 µg/ml in 50 mM HEPES-buffered saline (pH 7.6) containing 0.05% Tween 20, 1% BSA, 2 mM sodium orthovanadate, 1 mg of bacitracin per ml, and 1 mM PMSF and then with peroxidase-conjugated streptavidin. The peroxidase activity was determined colorimetrically by adding 100 µl of TMB. The reaction was stopped by the addition of 1.0 M H$_3$PO$_4$, and the absorbance was measured at 451 nm. The insulin receptor content was evaluated by comparing each sample to a standard curve. The IR standard was purified from NIH 3T3 cells transfected with the human IR cDNA by sequential affinity chromatography on wheat germ agglutinin-agarose and on agarose coupled with MA-20. The receptor concentration was measured by amino acid analysis (42).

RT-PCR. Reverse transcription-PCR (RT-PCR) for IR isoforms was carried out as previously described (47) with oligonucleotide primers spanning nucleotides 2229 to 2250 (5′-AAC-CAG-AGT-GAG-TAT-GAG-GAT-3′) and 2844 to 2865 (5′-CCG-TTC-CAG-AGC-GAA-GTG-CTT-3′) of the human IR. PCR amplification was carried out for 25 cycles of 20 s at 96°C, 30 s at 58°C, and 1.5 min at 72°C in a DNA thermal cycler (Perkin-Elmer Cetus). After electrophoresis of the PCR products, the 600- and 636-bp DNA fragments representing Ex11− and Ex11+ IR isoforms were analyzed by scanning densitometry and compared to the standards. Standard preparations were made with mRNA from NIH 3T3 cells transfected with cDNA of both IR isoforms mixed at various ratios and coamplified by RT-PCR. To verify that larger cDNA was really the IR-B isoform, RT-PCR products were subjected to BanI digestion. Only cDNA containing exon 11, the restriction site for the enzyme, was digested.

Incorporation of [^{3}H]thymidine or 5-bromo-2′-deoxyuridine into DNA. [^{3}H]thymidine incorporation in response to insulin or IGF-II was carried out as previously described (31). Cells were seeded in 24-multiwell plates and allowed to attach for 24 h. Complete medium was replaced with DMEM–0.1% BSA for 48 h to allow the cells to become quiescent. Growth factors were then added at the indicated concentrations. After 48 h, medium was removed and 0.5 µCi of [^{3}H]thymidine per ml was added for 2 h at 37°C. The cells were washed twice with ice-cold PBS (pH 7.4) and incubated with 1 ml of 10% ice-cold trichloroacetic acid for 30 min. The acid-insoluble fraction was solubilized in 0.5 ml of 0.1 N NaOH for 30 min at room temperature, and the incorporation of [^{3}H]thymidine into DNA was determined by scintillation counting. 5-Bromo-2′-deoxyuridine incorporation into cell nuclei, a further measurement of cell proliferation,
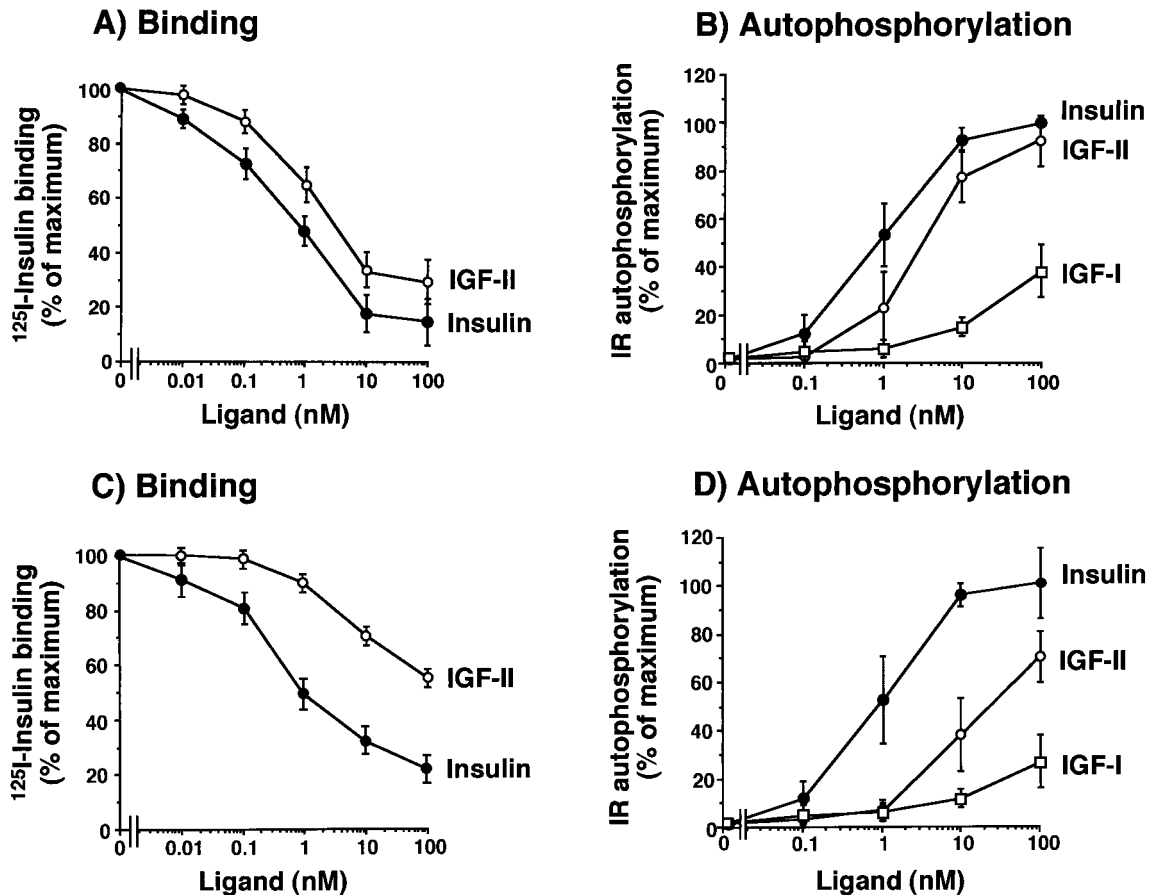
A) Binding

B) Autophosphorylation

C) Binding

D) Autophosphorylation

FIG. 1. IGF-II binds to and activates the IR-A (A and B) with a higher affinity than IR-B (C and D) in mouse R^- cells stably transfected with either isoform human cDNA. (A and C) Binding studies. Cells were grown to approximately 80% of confluence and, after 16 h of starvation in serum-free medium, were incubated with ^{125}I-insulin (10.0 pM) for a further 16 h at 4°C in the presence of increasing concentrations of either insulin or IGF-II. Then cell-associated radioactivity was measured in a γ-counter. The data represent the mean and standard error (SE) of six separate experiments. (B and D) IR autophosphorylation. Confluent cells were serum starved for 48 h in serum-free medium, exposed to either insulin or IGF-II at the indicated concentrations for 5 min, and solubilized in ice-cold lysis buffer. IR autophosphorylation was measured by an ELISA (3, 4) with a specific anti-IR antibody (MA-20) to immunocapture the IRs, and an antiphosphotyrosine biotin-conjugated antibody with streptavidin to phosphorylated tyrosines. The data represent the mean and standard error of six separate experiments.

was revealed by immunohistochemistry (Boehringer Mannheim), and the proportion of stained nuclei was scored under a microscope.

2-[³H]deoxyglucose uptake. 2-[³H]deoxyglucose uptake in response to insulin and IGF-II was carried out as previously described (30) with modifications. Cells were seeded in 24-multiwell plates and allowed to attach for 24 h. Complete medium was replaced with DMEM–0.1% BSA–5.5 mM glucose for 48 h. The cells were then washed three times with transport buffer (20 mM HEPES [pH 7.4], 120 mM NaCl, 1.2 mM $MgSO_4$, 2 mM $CaCl_2$, 2.5 mM KCl, 1 mM NaH_2PO_4, 1 mM sodium pyruvate) and incubated in this buffer for additional 90 min with either insulin or IGF-II at the concentrations indicated in the figure legends. Glucose transport was determined by incubation on ice for 10 min with 0.1 mM 2-deoxyglucose (4.0 μCi/ml; Amersham). Glucose transport was terminated by rapid removal of the buffer containing the radiolabeled glucose analogue and repeated washing with cold PBS, and cell-associated radioactivity was measured after cell monolayer solubilization with 0.1 N NaOH for 30 min at room temperature and scintillation counting.

Statistical analysis. Growth curves and 2-deoxyglucose incorporation in response to either insulin or IGF-II were compared by two-way analysis of variance. The proportions of nuclei labeled by bromodeoxyuridine in response to either insulin or IGF-II were compared by the use of contingency tables (χ^2 test). Statistical analysis was carried out with GraphPad software (Prism, London, United Kingdom).

RESULTS

IGF-II binds with high affinity and activates the tyrosine kinase activity of IR-A but not IR-B. To study the interaction of IGF-II with the IR isoforms, we used IR-transfected R^-

cells. R^- cells are mouse fibroblasts that are derived from animals with a targeted disruption of the IGF-I-R gene and thus do not express the IGF-I receptor (49). In addition, R^- cells, like NIH 3T3 fibroblasts, have low levels of the IR (approximately 5×10^3 receptors/cell or less). To study the specific interaction of IGF-II with each IR isoform, R^- cells were transfected with either IR-A or IR-B human cDNA, and approximately 5×10^5 receptors/cell were obtained. These engineered models, in which only one human IR isoform is present, allowed the direct examination of the interaction of IGF-II with each individual IR isoform.

In cells transfected with IR-A (R^-/IR-A cells), competition for labeled insulin binding revealed a high affinity of IGF-II for the IR-A, with a 50% effective concentration (EC_{50}) of 2.5 nM for IGF-II and 0.9 nM for insulin (ratio, 0.36) (Fig. 1A). Following stimulation of intact cell monolayers with either insulin or IGF-II, IR autophosphorylation was measured by ELISA. As expected from ligand binding data, low concentrations of IGF-II activated the human IR-A (EC_{50} of 3.0 ± 0.4 nM for IGF-II and 0.8 ± 0.2 nM for insulin [ratio, 0.27]) (Fig. 1B). Similar results were obtained when solubilized receptors were first immunopurified and then stimulated in vitro with either insulin or IGF-II (data not shown). These data indicated that

TABLE 1. Autophosphorylation of the two IR isoforms and IGF-I-R by insulin, IGF-II, or IGF-I

Cell line and receptor	EC_{50} (nM) for receptor autophosphorylation		
	Insulin	IGF-II	IGF-I
R⁻ cells			
IR-A	0.8 ± 0.2	3.0 ± 0.4	>30.0
IR-B	1.1 ± 0.4	24.0 ± 5.0	>30.0
IGF-I-R	>30.0	2.5 ± 1.0	1.6 ± 0.3
CHO cells			
IR-A	0.6 ± 0.1	3.8 ± 2.8	>30.0
IR-B	0.7 ± 0.2	30.0 ± 6.6	>30.0
IGF-I-R	>30.0	3.8 ± 0.4	2.1 ± 0.4
NIH 3T3 cells			
IR-A	0.7 ± 0.2	3.6 ± 0.7	>30.0
IR-B	0.8 ± 0.2	22.0 ± 4.0	>30.0

IR-A activation by IGF-II was an intrinsic property of the receptor and not the result of either interfering factors on the cell membrane or IGF-II binding proteins.

In contrast to results obtained with R⁻/IR-A cells, in R⁻ cells transfected with IR-B (R⁻/IR-B cells) IGF-II inhibited labeled insulin binding with a low affinity (EC_{50} of >20.0 nM for IGF-II and 1.0 nM for insulin) (Fig. 1C). Similarly, in these cells IGF-II activated IR-B autophosphorylation with approximately 5% the potency of insulin. This effect was observed in both intact cells and solubilized receptors (Fig. 1D). These results indicated that human IR-A (but not IR-B) is a high-affinity receptor for IGF-II.

Similar results in IR autophosphorylation were obtained when the two IR isoforms were also first transfected into either CHO cells or NIH 3T3 fibroblasts and then stimulated with either insulin or IGF-II and the IR isoform autophosphorylation was measured (Table 1). In contrast to IGF-II, IGF-I had low affinity for both IR isoforms.

IGF-II binds to and activates IR-A and IGF-I-R with a similar affinity. Because IGF-I-R is considered the physiological receptor for IGF-II, we compared the relative activity of IGF-II in binding to and stimulating the autophosphorylation of either IR-A or IGF-I-R. We transfected R⁻ cells with either IR-A or IGF-I-R cDNAs and found that they expressed a similar number of receptors (approximately 5×10^5 IRs/cell and 3.5×10^5 IGF-I-Rs/cell). Binding studies were then carried out to evaluate the ability of IGF-II to compete with either labeled insulin (in R⁻/IR-A cells) or labeled IGF-I (in R⁻/IGF-I-R cells). Competition/inhibition curves indicated that the EC_{50} of IGF-II was 2.5 ± 0.5 nM for IR-A and 2.0 ± 0.4 nM for IGF-I-R. We next evaluated the ability of IGF-II to stimulate receptor autophosphorylation in the same cells. The EC_{50} was 3.0 ± 0.4 nM for IR-A and 2.5 ± 1.0 nM for IGF-I-R (Table 1), indicating a very similar affinity of IGF-II for the two receptors. Similar results were obtained with CHO cells transfected with the same cDNAs: the EC_{50} of IGF-II was 3.8 ± 2.8 nM for IR-A and 3.8 ± 0.4 nM for IGF-I-R autophosphorylation (Table 1).

IGF-II interactions with IR-A are primarily mitogenic, whereas insulin interactions are primarily metabolic. The two ligands, insulin and IGF-II, induce different biological effects in target tissues, although a certain degree of overlap in their actions is well recognized (25). In general, insulin is important for metabolic activities whereas IGF-II is important for cell growth and survival. This difference in the biological effects has been previously attributed to ligand interaction with different receptors, i.e., insulin with IR and IGF-II with IGF-I-R.

We then evaluated cells expressing IR-A to determine whether IGF-II elicited biological effects that were similar to those of insulin (Fig. 2). In R⁻ cells transfected with IR-A, insulin was more potent than IGF-II ($P = 0.038$) in stimulating 2-deoxyglucose uptake (Fig. 2C). In contrast, IGF-II was significantly more potent than insulin in inducing growth, as measured by either [³H]thymidine ($P < 0.0001$) or 5-bromo-2′-deoxyuridine ($P = 0.039$) incorporation (Fig. 2A and B). These data indicated that IR-A stimulation by either insulin or IGF-II generates different biological effects.

Intracellular signaling following IR-A activation by either insulin or IGF-II is different. Activation of the insulin receptor β-subunit tyrosine kinase domain by ligand binding to the α-subunit is followed by tyrosine phosphorylation of docking protein including the IRS protein family and Shc (20). IRS and Shc recruit and activate different signal generators (2, 36). These generators include the lipid PI3-kinase and GTPase regulators (such as ras). They then activate cytosolic effectors including ERK1 and ERK2 (p42 and p44 mitogen-activated protein kinase, respectively), which are believed to represent a major mitogenic pathway (2, 36).

To identify possible differences in intracellular signaling pathways (46, 59) when IR-A was activated by either insulin or IGF-II, we exposed R⁻ cells expressing IR-A (R⁻/IR-A cells) to each ligand and measured the activation of IR-A itself, and the intracellular substrates IRS-1, IRS-2, Shc, PI3-kinase, ERK1 kinase, and ERK2 kinase. Differences between insulin and IGF-II were found in all signaling molecules. IR-A autophosphorylation, when stimulated by insulin, peaked at 1 to 2 min and then declined to approximately 75% of maximum at 60 min (Fig. 3A). In contrast, when stimulated with IGF-II, IR-A autophosphorylation reached a smaller peak at 5 min and thereafter declined to approximately 85% of the maximum at 60 min (Fig. 3A). A similar pattern was observed when the tyrosine phosphorylation of substrates IRS-1 and IRS-2 was measured. Phosphorylation of both substrates peaked at 1 to 2 min after the addition of insulin, whereas there was a lower and delayed elevation (plateau at 2 to 5 min) after the addition of IGF-II (Fig. 3B and C). The peak stimulation of both substrates was higher after insulin addition but then rapidly declined. Between 5 and 60 min, the activation level was similar for both insulin and IGF-II. Although in R⁻/IR-A cells the relative abundance of IRS-1 and IRS-2 (as measured by Western blotting) was similar (data not shown), both ligands preferentially activated IRS-2. The IRS-2/IRS-1 activation ratio during the first 10 min of stimulation ranged from 1.6 to 2.3 in response to insulin and 2.2 to 3.1 in response to IGF-II. In response to insulin, maximal Shc phosphorylation (calculated as 52-kDa Shc isoform tyrosine phosphorylation) occurred within 3 min and was sustained up to 60 min. In contrast, for IGF-II we observed a value that peaked at 5 min and then slowly declined and reached basal level at 60 min (Fig. 3D). For PI3-kinase activity (Fig. 4A), maximal activity was lower with IGF-II (less than 50% of that observed after insulin) and delayed. Approximately 85% of the PI3-kinase activity was recovered in immunoprecipitates with the anti-IRS-2 antibody (rather than the anti-IRS-1 antibody) immunoprecipitates for both ligands. Maximal tyrosine phosphorylation of ERK1 and ERK2 was slightly reduced and delayed after IGF-II stimulation compared to insulin stimulation (Fig. 4B). ERK1 and ERK2 activation was also more transient after IGF-II than after insulin stimulation and approached basal levels at 20 min.

Human fetal cells and tissues preferentially express IR-A compared with adult tissues. To investigate whether increased IR-A expression in fetal cells could explain the previous findings of the presence of an "atypical" IR with high affinity for
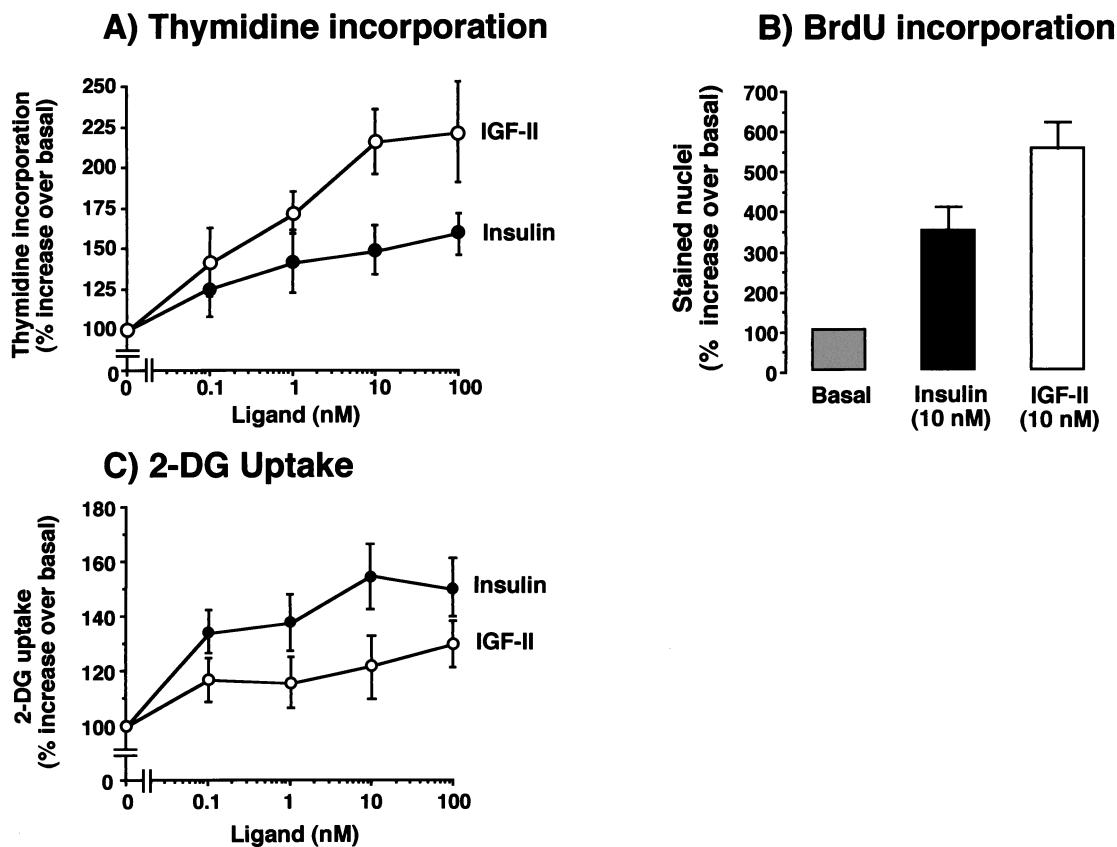
A) Thymidine incorporation

B) BrdU incorporation

C) 2-DG Uptake

FIG. 2. Mitogenic and metabolic effects of IR-A activated by either insulin or IGF-II. Mouse R^{−} cells, stably transfected with the IR-A cDNA (R[−]/IR-A), were exposed to either insulin or IGF-II. (A) [^{3}H]thymidine incorporation. Cells grown in 24-multiwell plates were serum starved for 48 h in serum-free medium and then exposed to either insulin or IGF-II for a further 48 h at the indicated concentrations. At the end of the stimulation, [^{3}H]thymidine (0.5 μCi/well) was added for 2 h at 37°C. After cell solubilization, incorporation of [^{3}H]thymidine into nuclei, an index of cell proliferation, was measured in the acid-insoluble fraction in a scintillation counter. Data represent the mean and standard error of five separate experiments. (B) Bromodeoxyuridine incorporation. Parallel experiments were carried out by measuring the percentage of 5-bromodeoxyuridine (BrdU) labeled nuclei of cells exposed to 10 nM insulin or IGF-II. Data represent the mean and standard error of five separate experiments. (C) 2-Deoxyglucose transport. Cells grown in 24-multiwell plates were incubated in 5.5 mM glucose for 48 h, and then either insulin or IGF-II was added for 90 min at the indicated concentrations. 2-Deoxyglucose (2-DG) (0.1 mM; 0.2 μCi/ml) was added, and cells were incubated on ice for 10 min. After cell solubilization, 2-deoxyglucose uptake, an index of the metabolic effect, was measured in a scintillation counter. Data represent the mean and standard error of five separate experiments.

IGF-II in cells of fetal origin (18), we measured IR-A expression by RT-PCR analysis in samples of several human fetal tissues, including brain, muscle, liver, kidney, and fibroblasts, and compared these values to those obtained in paired adult tissues. In all fetal tissues except brain (Table 2), the relative abundance of the IR-A isoform was higher than in adult tissues. In muscle, liver, and kidney, the proportion of IR-A isoform ranged from 45.5 to 52.5% in fetal tissues and decreased to 28.5 to 45.5% in adult tissues. Dermal fibroblasts of either fetal or adult origin (three samples from each source) were cultured in monolayers. The relative abundance of IR-A was 72 to 84% in fetal fibroblasts and 20 to 39% in adult fibroblasts (Fig. 5). These data suggest, therefore, that during fetal life most tissues predominantly express IR-A and that splicing of exon 11 of the IR is developmentally regulated (15).

To evaluate the role of IGF-II/IR-A interaction in human fetal cells (i.e., whether the increased IR-A proportion could determine IGF-II signaling through the IR), we next carried out IR binding and IR autophosphorylation studies with cultured human fetal and adult fibroblasts. Unlabeled IGF-II inhibited ^{125}I-insulin binding and activated IR autophosphorylation with a 10-fold-higher affinity in fetal than in adult fibroblasts (Fig. 6). For both inhibition of ^{125}I-insulin binding

and stimulation of IR autophosphorylation, the EC$_{50}$ was 8 to 10 nM IGF-II in fetal fibroblasts and >100 nM IGF-II in adult fibroblasts. IGF-I bound to the two IR isoforms with similar low affinities (EC$_{50}$ > 100 nM).

Human cancers preferentially express IR-A in comparison with normal tissues. Since many cancers express IGF-II and other fetal proteins (e.g., carcinoembryonic antigen, alpha-fetoprotein), we investigated the relative abundance of the IR-A in a limited series of surgical specimens from the most common human cancers, including breast, lung, and colon. These specimens were obtained together with specimens of normal tissue, and IR-A and IR-B isoform expression was determined by RT-PCR. In breast and colon cancer, the relative abundance of IR-A was significantly higher than in normal tissues ($P = 0.005$ and $P = 0.009$, respectively), with median values ranging from 68 to 73% in cancer tissue and 35 to 43% in normal tissue (Table 3). Especially in breast cancer, the average IR content was also significantly higher in the malignant tissues than in normal tissues (Table 3). Thus, in some tumors, the combined effects of IR overexpression and the relative abundance of IR-A increased the absolute content of IR-A.

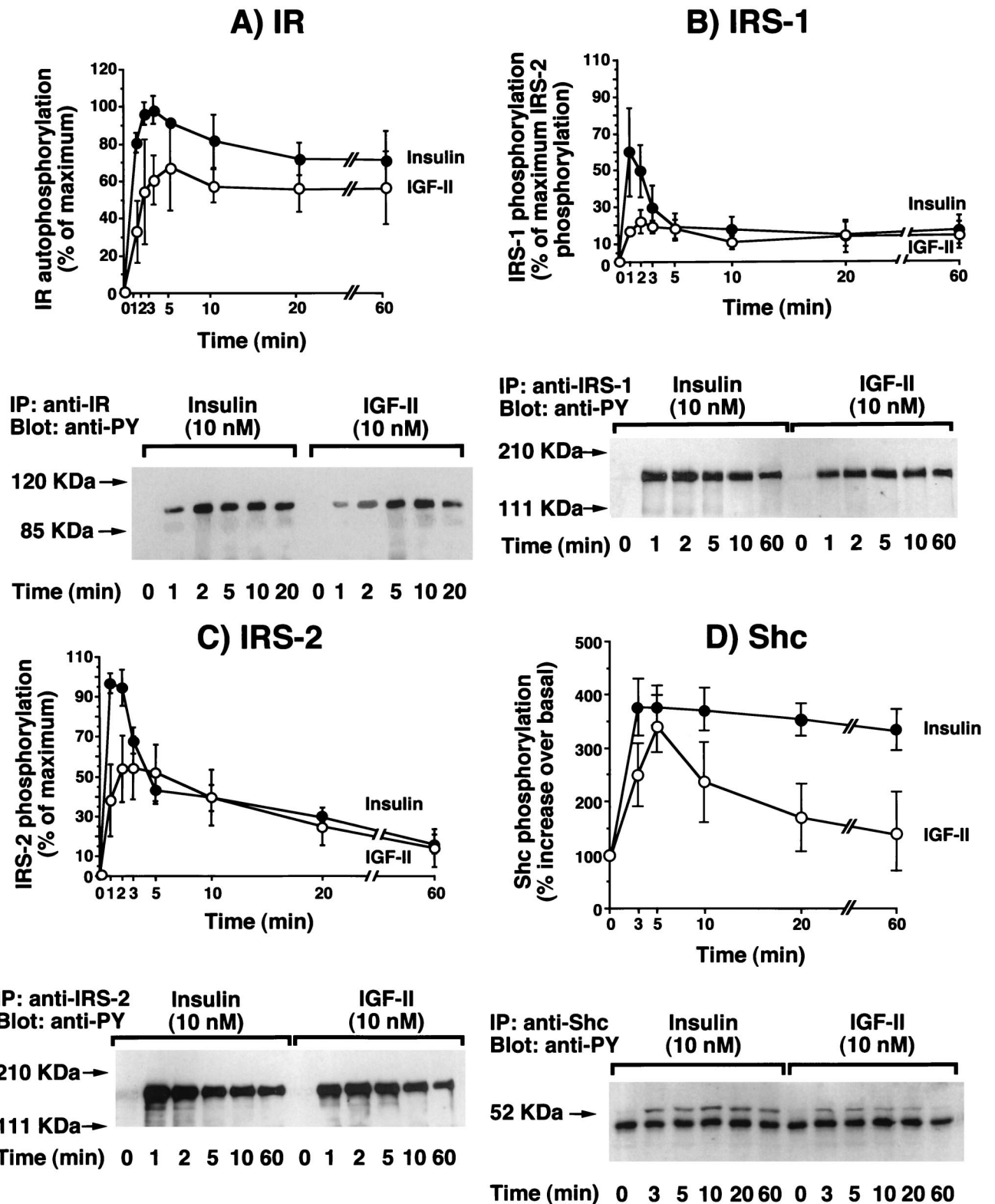We then evaluated the ability of IGF-II to activating IR

FIG. 3. Time courses of IR-A phosphorylation and post-receptor protein phosphorylation of IRS-1, IRS-2, and Shc in mouse R⁻ cells transfected with IR-A cDNA and exposed to either insulin or IGF-II. Confluent cells were serum starved for 48 h in serum-free medium, exposed to 10 nM either insulin or IGF-II for the indicated times, and solubilized in lysis buffer. After protein quantitation, aliquots were used for ELISA and Western blot measurements. (A) IR autophosphorylation was quantitated by a specific ELISA (top) and detected by Western blotting (bottom). Monoclonal antibody MA-20 was used to immunocapture phosphorylated IR. (B) IRS-1 phosphorylation was measured by a specific ELISA (top) and detected by Western blotting (bottom). A polyclonal anti-IRS-1 antibody was used to immunocapture phosphorylated IRS-1. (C) IRS-2 phosphorylation was quantitated by a specific ELISA (top) and detected by Western blotting (bottom). A polyclonal anti-IRS-2 antibody was used to immunocapture phosphorylated IRS-2. (D) The 52-kDa Shc isoform phosphorylation was detected by Western blotting (bottom) and quantitated by densitometric scanning with Adobe Photoshop and NIH Image software (top). A polyclonal anti-Shc antibody was used to immunocapture phosphorylated Shc. Tyrosine phosphorylation of these proteins was revealed by using an antiphosphotyrosine (anti-PY) antibody biotin conjugated for the ELISAs. The top panels show the mean and standard error of three separate experiments (except for Shc, where five experiments were carried out); the bottom panels show a representative experiment of three (five for Shc). IP, immunoprecipitation.
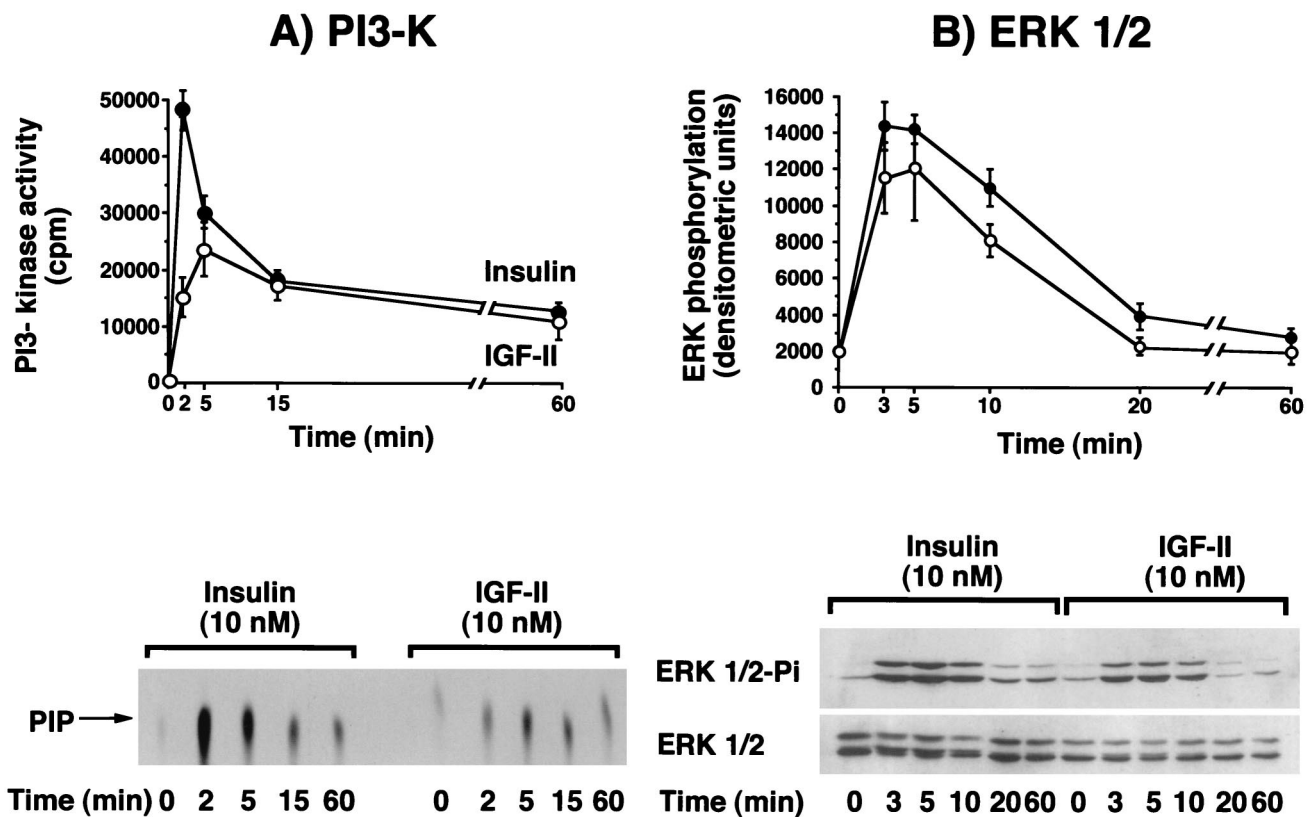
A) PI3-K

B) ERK 1/2

FIG. 4. Time course of either insulin or IGF-II in stimulating PI3-K activity and ERK1 and ERK2 phosphorylation in R⁻ cells overexpressing IR-A. Confluent cells were serum starved for 48 h in serum-free medium and then treated with 10 nM insulin or IGF-II for the indicated times. The cells were solubilized in ice-cold lysis buffer, and after protein quantitation, samples were subjected to either immunoprecipitation or Western blotting. (A) PI3-kinase activity was evaluated in antiphosphotyrosine immunoprecipitates by measuring ³³P incorporation into PI, as indicated in Materials and Methods. The reaction mixture was spotted onto a silica gel plate and subjected to radioactivity counting of PIP spots (top) (mean and standard error of three separate experiments) and autoradiography (bottom). (B) ERK1 and ERK2 phosphorylation was studied by Western blotting with an anti-phosphorylated ERK-specific antibody, and the filter was reprobed with anti-ERK1 and anti-ERK2 polyclonal antibody (New England Biolabs). The top panel shows densitometric scanning (mean and standard error of four separate experiments), using Adobe Photoshop and NIH Image software; the bottom panel shows a representative experiment.

autophosphorylation in cancer tissues and compared these data with those obtained for normal tissues. IRs were immunopurified from tissue lysates by adsorption to Maxisorb plates precoated with MA-20 antibody and stimulated with either insulin or IGF-II at different concentrations. IR autophosphorylation was then measured as described in Materials and Methods. The IGF-II potency (data not shown), calculated as the percentage of insulin ED_{50} relative to the IGF-II ED_{50} for stimulation of IR autophosphorylation, was correlated with the proportion of IR-A expression ($r = 0.51$, $P = 0.001$; Spearman rank correlation).

These observations indicated that in some cancers, locally

produced IGF-II may bind to and activate the IR with high affinity. This may be biologically relevant when IR is overexpressed and IR-A is the predominant isoform.

DISCUSSION

The present study demonstrates that IR-A is a physiological receptor for IGF-II. Previously it was believed that most, if not all, biological effects of IGF-II in cells were mediated by IGF-

TABLE 2. Proportion of IR-A mRNA in adult and fetal normal human tissues and in cultured dermal fibroblasts

Tissue or cell type	Proportion (%) of IR-A[a] in:		P
	Fetal tissue	Adult tissue	
Brain	51.5 ± 3.5	52.0 ± 2.5	0.627
Kidney	52.5 ± 2.5	45.5 ± 0.5	0.008
Muscle	47.0 ± 2.0	35.0 ± 5.0	0.017
Liver	45.5 ± 0.5	28.5 ± 1.5	0.001
Fibroblasts	78.2 ± 6.3	29.6 ± 9.2	0.001

[a] as determined by RT-PCR (mean ± standard error of triplicate measurements).
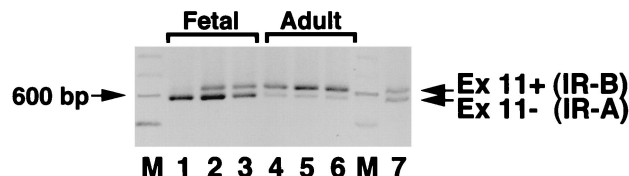

FIG. 5. IR isoform expression is different in fetal and adult human fibroblasts, as measured by RT-PCR. RNA was extracted by the acidic-phenol method from cultured fibroblasts obtained from three fetuses and three adult subjects, and RT-PCR of IR isoform expression was carried out for 25 cycles. After electrophoresis in 2% agarose gel, ethidium bromide-stained DNA fragments (600 and 636 bp for IR-A and IR-B, respectively) were quantitated by scanning densitometry with Adobe Photoshop and NIH Image software. Fetal fibroblasts (lanes 1 to 3) predominantly expressed the IR-A isoform, whereas adult fibroblasts (lanes 4 to 6) predominantly expressed the IR-B isoform. A mixture of cDNA (1:1) of the two isoforms was coamplified and used as positive control (lane 7). A representative experiment is shown.

A) Binding

B) Autophosphorylation

C) Binding
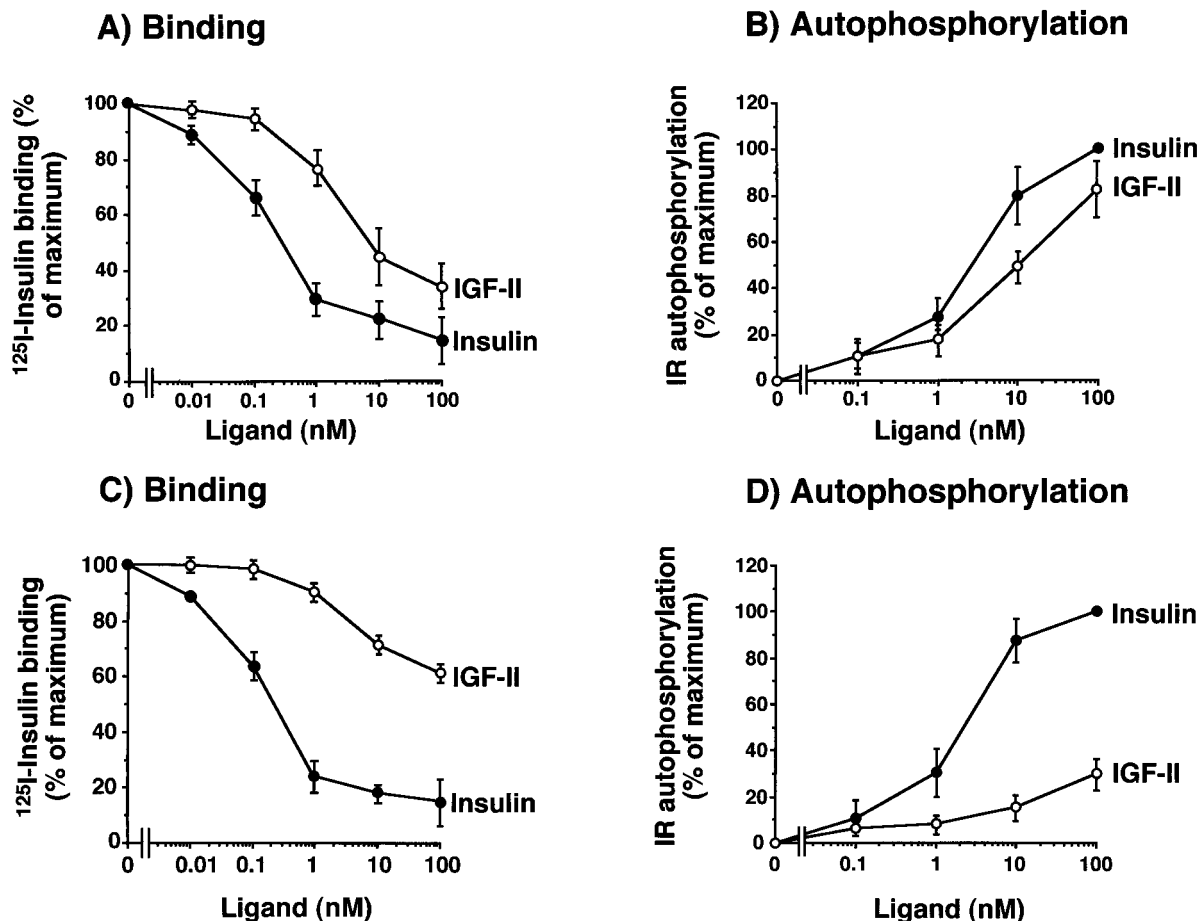
D) Autophosphorylation

FIG. 6. IGF-II binds to and activates IR with high affinity in fetal human fibroblasts (A and B) but not in adult human fibroblasts (C and D). (A and C) Binding studies. Fibroblasts from three adult and three fetal subjects were grown to approximately 80% confluence and, after 16 h of starvation in serum-free medium, incubated with ^{125}I-insulin (10.0 pM) for a further 16 h at 4°C in the presence of increasing concentrations of either insulin or IGF-II. Cell-associated radioactivity was then measured in a γ-counter. The results are the mean and standard error of three separate experiments with fibroblasts from different subjects. (B and D) IR autophosphorylation. Confluent fibroblasts were serum starved for 24 h in serum-free medium and then exposed to either insulin or IGF-II at the indicated concentrations for 5 min. After solubilization in ice-cold lysis buffer, IR autophosphorylation was measured by an ELISA with a specific anti-IR antibody (MA-20) to immunocapture the IRs and an antiphosphotyrosine biotin-conjugated antibody with streptavidin to readout phosphorylated tyrosines. The results are the mean and standard error of three separate experiments with fibroblasts from different subjects.

I-R. IGF-II-R, which also binds mannose-6-phosphate resi-dues, is devoid of tyrosine kinase activity and is not believed to have either metabolic or mitogenic signaling potential. Most studies have indicated that the IR, which is homologous to the

TABLE 3. Proportion of IR-A mRNA and total IR content in normal and cancer specimens from human breast, lung, and colon

Tissue (no. of specimens)	Proportion (%) of IR-A[a]		P value	IR content (ng/0.1 μg of protein)
	Range	Median		
Breast cancer ($n = 12$)	40–80	73		3.2 ± 1.8
Normal breast ($n = 12$)	30–50	43	0.005	0.5 ± 0.3
Lung cancer ($n = 6$)	30–60	53		1.1 ± 0.3
Normal lung ($n = 6$)	30–55	39	0.065	0.5 ± 0.1
Colon cancer ($n = 10$)	65–80	68		1.8 ± 0.5
Normal colon ($n = 10$)	30–65	35	0.01	1.3 ± 0.4

[a] As determined by RT-PCR.
[b] Wilcoxon signed-rank test.

IGF-I-R, binds IGF-II with a relatively low affinity (1 to 5% that of insulin) (45). However, there is evidence that in certain instances the IR can bind IGF-II with high affinity. "Atypical" IRs, which bind IGF-II with unusually high affinity, have been found in IM-9 lymphoblasts, immature erythrocytes (18), and fetal tissues (including human placenta and brain, and chicken embryo fibroblasts) (19). Furthermore, other studies suggest that during mouse fetal development, the growth promoting effect of IGF-II is mediated in part by signaling through the IR (28). By analyzing mouse dwarfing phenotypes resulting from targeted mutagenesis of the IGF-I and IGF-II genes and the cognate IGF-I-R gene, Efstratiadis and coworkers demon-strated that this signaling system is important for the growth of the embryo (9, 27). It was also observed that while IGF-I interacts exclusively with the IGF-I-R, IGF-II recognizes an additional receptor, because growth retardation in embryos lacking both IGF-I-R and IGF-II was more severe than in single IGF-I-R mutants but similar to that obtained in double mutants lacking both IGF-I-R and IR (28). Finally, it has been reported that IGF-II can stimulate proliferation not only through the IGF-I-R but also through the IR (34). Studies with R$^-$ cells indicate that these cells fail to proliferate in response

to growth factors (49). However, when cells are transfected with and overexpress the IR, they are able to grow in serum-free medium supplemented with either insulin or IGF-II but not with IGF-I (32). In these studies, however, the IR isoform used was not reported.

In the present study, employing R⁻ cells transfected with either IR-A or IR-B cDNAs, we were able to investigate the interaction of IGF-II with the two IR isoforms without interference by the IGF-I-R. We observed that while IGF-I bound with low affinity to both IR isoforms. IGF-II was bound by IR-A with relatively high affinity (30 to 40% that of insulin). We also found that IR-A but not IR-B was autophosphorylated by IGF-II with a similar high affinity. The same results were obtained by using either intact cells or solubilized receptors, indicating that they resulted from an intrinsic characteristic of IR-A and not from the presence of other cellular factors. By using R⁻ cells transfected with the IGF-I-R cDNA, we observed that the affinity of IGF-II for IR-A was very similar to its affinity for IGF-I-R.

The reason why IR-A binds IGF-II with a higher affinity than does IR-B is unknown. Recent studies have suggested that the major insulin binding determinants reside within the first 468 amino acids and residues 704 to 716 of the IR molecule (24). However, the 12 carboxyl-terminal amino acids (amino acids 718 to 729, encoded by exon 11) may influence ligand binding, since IR-A binds insulin with a slightly higher affinity than does IR-B (60). It is possible that these 12 C-terminal amino acids hinder IGF-II binding to IR-B. Structural analysis of IR binding sites by X-ray crystallography with IR fragments differing in either the presence or absence of the 12 amino acids encoded by exon 11 should provide a better understanding of the different binding affinity of IGF-II for the two IR isoforms.

Of major interest is the observation that in R⁻ cells expressing IR-A, IGF-II (in contrast to insulin) predominantly elicited mitogenic effects. Although the predominant effects of IR activation by insulin are metabolic, there is evidence that mitogenic effects may also be elicited (10, 25, 31, 34). In R⁻/IR-A cells, when glucose transport was studied, insulin had a greater effect on this metabolic function than did IGF-II. In contrast, when thymidine incorporation was studied, IGF-II had a greater effect than insulin. The specificity of a receptor signaling may be regulated in different ways. The IR, like other tyrosine kinase receptors, interacts with a number of intracellular signaling molecules. After autophosphorylation, the IR phosphorylates docking proteins like IRS-s and Shc (2, 20, 36). These proteins then activate downstream signaling pathways, including PI3-kinase, ERK1, and ERK2 (2, 36). When we analyzed these docking proteins and signaling pathways, we observed quantitative and temporal differences when IR-A was activated by either insulin or IGF-II. Both IRS-1 and the Shc pathways were less intensely and more transiently activated after IGF-II than after insulin stimulation; these data do not support the possibility that these pathways are responsible for the increased mitogenic effect of IGF-II unless one hypothesizes that a more transient activation of certain substrates (e.g., ERK) may lead to a more mitogenic signal, as previously suggested (39, 54, 57). Alternatively, it is possible that other pathways (e.g., ras) are involved. However, these observations indicate that a site of selectivity for metabolic versus mitogenic signaling may occur at the ligand binding domain. Similar observations have already been reported for other receptors, such as the epidermal growth factor receptor (26). Also in this case, different ligands may elicit different receptor activation and postreceptor signaling (21). It is also known that insulin analogs with different binding properties may affect both sig-

naling specificity and the timing of events downstream of receptor binding (17, 50).

Also, our studies in humans indicate that, as in mice (1, 15, 18, 22), IR isoform expression is regulated by development. When we examined human fetal tissues and compared the relative prevalence of IR-A in these tissues with respect to that in adult tissues, we observed a clear shift from IR-A to IR-B in muscle, liver, and kidney. In human cultured fetal fibroblasts, the relative expression of IR-A was higher than in adult fibroblasts. As in R⁻ cells expressing IR-A, human fetal fibroblasts IGF-II bound to the IR with high affinity and had potent effects in stimulating IR autophosphorylation.

IR isoform expression is also regulated by differentiation (15, 22). Many cancer cells dedifferentiate and acquire a more fetal phenotype, expressing proteins and antigens typical of fetal cells. In the small series of tumors reported herein, we found that IR-A is the predominant isoform in breast and colon cancers but not in the corresponding normal tissues. On average, the total IR protein content was also increased in these cancers. In tumors that predominantly expressed IR-A, IGF-II was a relatively potent activator of the IR. Various tumor cells express IGF-II. The preferential IR-A expression in certain cancers may therefore activate an autocrine/paracrine loop whenever IGF-II is locally produced.

We have recently confirmed these data in a larger series of breast carcinomas and in cultured breast cell lines and have observed that a proportion of these cancer tissues and cells also express IGF-II (48). In these conditions, IGF-II is considered to be a major factor for cancer cell proliferation and survival via autocrine or paracrine pathways. Further studies are needed to ascertain whether other cancers, including those typically expressing large quantities of IGF-II (e.g., rhabdomyosarcomas, adrenal cancers, and Wilms' tumors) (6, 8, 37, 38, 41, 51, 56, 61, 62) also overexpress IR-A.

The molecular mechanisms involved in the developmental and differentiation regulation of the alternative splicing process of the IR gene are not clear. It has recently been reported that specific regions in intron 10 and exon 11 of the IR gene are involved in this process (23). In studies carried out with HepG2 human hepatoma cells, which differentiate and predominantly express IR-B after stimulation with glucocorticoids (22), both splicing enhancer sequences and inhibitory regions have been identified in intron 10 and splice site selection sequences have been identified in the IR gene exon 11 (23). Modified alternative splicing for a variety of proteins has been found in proliferating cells and in cancer cells. In these models, the change in the splicing pattern of pre-mRNAs occurs simultaneously with a change in the expression level of splicing factors of the SR family of phosphoproteins which bind pre-mRNA very early during spliceosome assembly and determine the 5′-splice-site choice during the splicing reaction. SR protein activity is modulated by antagonist proteins, such as heterogeneous ribonucleoproteins: a predominance of these heterogeneous ribonucleoproteins favors distal 5′-splice-site choices and exon skipping (29). The opposite occurs with increased SR levels. Intracellular factors (like cyclic AMP) (44) and extracellular conditions (like pH) (5, 14) are also known to influence the alternative splicing pattern of different proteins. The regulators of IR gene exon 11 skipping are not known and need to be investigated, since they enable the IR gene to encode receptor protein isoforms with different functions.

In conclusion, the present study demonstrates that the IR isoform A is a physiological receptor for IGF-II and explains both the previously described data with "atypical" IRs with high-affinity IGF-II binding (18, 19, 34) and the role of the IR in fetal development (11, 28). Also, the present findings may

shed new light on the role of the IR in cancer biology. IRs are often overexpressed in cancer cells (13, 31, 43), and the prevalent expression of IR-A may provide a selective growth advantage to malignant cells in tumors that also produce IGF-II.

ACKNOWLEDGMENTS

REFERENCES

1. **Alexandrides, T., A. C. Moses, and R. J. Smith.** 1989. Developmental expression of receptors for insulin, insulin-like growth factor I (IGF-I), and IGF-II in rat skeletal muscle. Endocrinology **124:**1064–1076.
2. **Avruch, J.** 1998. Insulin signal transduction through protein kinase cascades. Mol. Cell. Biochem. **182:**31–48.
3. **Belfiore, A., A. Costantino, F. Frasca, G. Pandini, R. Mineo, P. Vigneri, I. D. Goldfine, B. A. Maddux, and R. Vigneri.** 1996. Overexpression of membrane glycoprotein PC-1 in MDA-MB 231 breast cancer cells is associated with inhibition of insulin receptor tyrosine kinase activity. Mol. Endocrinol. **10:**1318–1326.
4. **Boge, A., and R. A. Roth.** 1995. A non radioactive assay for the insulin receptor tyrosine kinase: use in monitoring receptor tyrosine kinase activity after activation of overexpressed protein kinase C alpha and high glucose treatment. Anal. Biochem. **231:**323–332.
5. **Borsi, L., E. Balza, B. Gaggero, G. Alemanni, and L. Zardi.** 1995. The alternative splicing pattern of the tenascin-C pre-mRNA is controlled by the extracellular pH. J. Biol. Chem. **270:**6243–6245.
6. **Boulle, N., A. Logie, C. Gicquel, L. Perin, and Y. Le Bouc.** 1998. Increased levels of insulin-like growth factor II (IGF-II) and IGF-binding protein-2 are associated with malignancy in sporadic adrenocortical tumors. J. Clin. Endocrinol. Metab. **83:**1713–1720.
7. **Carrascosa, J. M., B. Vogt, A. Ullrich, and H. U. Haring.** 1991. Activation of phosphatidylinositol-3-kinase by insulin is mediated by both A and B human insulin receptor types. Biochem. Biophys. Res. Commun. **174:**123–127.
8. **Cullen, K. C., M. E. Lippman, D. Chow, S. Hill, N. Rosen, and J. A. Zwiebel.** 1992. Insulin-like growth factor-II overexpression in MCF-7 cells induces phenotypic changes associated with malignant progression. Mol. Endocrinol. **6:**91–100.
9. **DeChiara, T. M., A. Efstratiadis, and E. J. Robertson.** 1990. A growth-deficiency phenotype in heterozygous mice carrying an insulin-like growth factor II gene disrupted by targeting. Nature **345:**78–80.
10. **De Meyts, P.** 1994. The structural basis of insulin and insulin-like growth factor-I receptor binding and negative co-operativity, and its relevance to mitogenic versus metabolic signalling. Diabetologia **37:**S135–S148.
11. **Efstratiadis, A.** 1996. Genetics of growth: developmental roles of IGF and insulin receptors. Exp. Clin. Endocrinol. Diabetes **104**(Suppl. 2):4–6.
12. **Forsayeth, J. R., A. Montemurro, B. A. Maddux, R. DePirro, and I. D. Goldfine.** 1987. Effect of Monoclonal antibodies on human insulin receptor autophosphorylation, negative cooperativity, and down-regulation. J. Biol. Chem. **262:**4134–4140.
13. **Frittitta, L., L. Sciacca, R. Catalfamo, A. Ippolito, P. Gangemi, V. Pezzino, S. Filetti, and R. Vigneri.** 1999. Functional insulin receptors are overexpressed in thyroid tumors. Is this an early event in thyroid tumorigenesis? Cancer **85:**492–498.
14. **Gerweck, L. E., and K. Seetharaman.** 1996. Cellular pH gradient in tumor *versus* normal tissue: potential exploitation for the treatment of cancer. Cancer Res. **56:**1194–1198.
15. **Giddings, S. J., and L. R. Carnaghi.** 1992. Insulin receptor gene expression during development: developmental regulation of insulin receptor mRNA abundance in embryonic rat liver and yolk sac, developmental regulation of insulin receptor gene splicing, and comparison to abundance of insulin-like growth factor 1 receptor mRNA. Mol. Endocrinol. **6:**1665–1672.
16. **Gliozzo, B., C. K. Sung, P. L. Scalia, V. Papa, F. Frasca, L. Sciacca, F. Giorgino, G. Milazzo, I. D. Goldfine, R. Vigneri, and V. Pezzino.** 1998. Insulin-stimulated cell growth in IRS-1 deficient ZR-75-1 cells is mediated by a phosphatidylinositol-3 kinase independent pathway. J. Cell. Biochem. **70:**268–280.
17. **Hansen, B. F., G. M. Danielsen, K. Drejer, A. R. Sorensen, F. C. Wiberg, H. H. Klein, and A. G. Lundemose.** 1996. Sustained signalling from the insulin receptor after stimulation with insulin analogues exhibiting increased mitogenic potency. Biochem. J. **315:**271–279.
18. **Hintz, R. L., A. V. Thorsson, G. Enberg, and K. Hall.** 1984. IGF-II binding on human lymphoid cells: demonstration of a common high affinity receptor for insulin like peptides. Biochem. Biophys. Res. Commun. **118:**774–782.
19. **Jonas, H. A., J. D. Newman, and L. C. Harrison.** 1986. An atypical insulin receptor with high affinity for insulin-like growth factors copurified with placental insulin receptors. Proc. Natl. Acad. Sci. USA **83:**4124–4128.
20. **Kao, A. W., S. B. Waters, S. Okada, and J. E. Pessin.** 1997. Insulin stimulates the phosphorylation of the 66- and 52-kilodalton Shc isoforms by distinct pathways. Endocrinology **138:**2474–2480.
21. **Korc, M., C. A. Haussler, and N. S. Trookman.** 1987. Divergent effects of epidermal growth factor and transforming growth factors on a human endometrial carcinoma cell line. Cancer Res. **47:**4909–4914.
22. **Kosaki, A., and N. J. Webster.** 1993. Effect of dexamethasone on the alternative splicing of the insulin receptor mRNA and insulin action in HepG2 hepatoma cells. J. Biol. Chem. **268:**21990–21996.
23. **Kosaki, A., J. Nelson, and N. J. G. Webster.** 1998. Identification of intron and exon sequences involved in alternative splicing of insulin receptor pre-mRNA. J. Biol. Chem. **273:**10331–10337.
24. **Kristiensen, C., F. C. Wiberg, L. Schaffer, and A. S. Andersen.** 1998. Expression and characterization of a 70 kDa fragment of the insulin receptor that binds insulin. J. Biol. Chem. **273:**17780–17786.
25. **Lamothe, B., A. Bandry, C. T. Christoffersen, P. De Meyts, J. Jami, D. Bucchini, and R. L. Joshi.** 1998. Insulin receptor-deficient cells as a new tool for dissecting complex interplay in insulin and insulin-like growth factors. FEBS Lett. **426:**381–385.
26. **Lipeski, L. E., J. M. Boylan, and P. A. Gruppuso.** 1996. A comparison of epidermal growth factor receptor-mediated mitogenic signaling in response to transforming growth factor alpha and epidermal growth factor in cultured fetal rat hepatocytes. Biochem. Mol. Biol. Int. **39:**975–983.
27. **Liu, J.-P., A. Baker, A. S. Perkins, E. J. Robertson, and A. Efstratiadis.** 1993. Mice carrying null mutations of the genes encoding insulin-like growth factor I (Igf-1) and type 1 IGF receptor (Igf1r). Cell **75:**59–72.
28. **Louvi, A., D. Accili, and A. Efstratiadis.** 1997. Growth promoting interaction of IGF-II with the insulin receptor during mouse embryonic development. Dev. Biol. **189:**33–48.
29. **Mayeda, A., D. M. Helfman, and A. R. Krainer.** 1993. Modulation of exon skipping and inclusion by heterogeneous nuclear ribonucleoprotein A1 and pre-mRNA splicing factor SF2/ASF. Mol. Cell. Biol. **13:**2993–3001.
30. **Mayor, P., L. Maianu, and T. Garvey.** 1992. Glucose and insulin chronically regulate insulin action via different mechanisms in BC$_3$H1 myocites. Diabetes **41:**274–284.
31. **Milazzo, G., F. Giorgino, G. Damante, C. K. Sung, M. R. Stampfer, R. Vigneri, I. D. Goldfine, and A. Belfiore.** 1992. Insulin receptor expression and function in human breast cancer cell lines. Cancer Res. **52:**3924–3930.
32. **Miura, M., E. Surmacz, J.-L. Burgaud, and R. Baserga.** 1995. Different effects on mitogenesis and transformation of a mutation at tyrosine 1251 of the insulin-like growth factor I receptor. J. Biol. Chem. **270:**22639–22644.
33. **Moller, D. E., A. Yokota, J. F. Caro, and J. S. Flier.** 1989. Tissue-specific expression of two alternatively spliced insulin receptor mRNAs in man. Mol. Endocrinol. **3:**1263–1269.
34. **Morrione, A., B. Valentinis, S. Xu, G. Yumet, A. Louvi, A. Efstratiadis, and R. Baserga.** 1997. Insulin-like growth factor II stimulates cell proliferation through the insulin receptor. Proc. Natl. Acad. Sci. USA **94:**3777–3782.
35. **Mosthaf, L., K. Grako, T. J. Dull, L. Coussens, A. Ullrich, and D. A. McClain.** 1990. Functionally distinct insulin receptors generated by tissue-specific alternative splicing. EMBO J. **8:**2409–2413.
36. **Myers, M. G., Jr., and M. F. White.** 1996. Insulin signal transduction and the IRS proteins. Annu. Rev. Pharmacol. Toxicol. **36:**615–658.
37. **Nonomura, N., K. Nishimura, T. Miki, N. Kanno, Y. Kojima, M. Yokoyama, and A. Okuyama.** 1997. Loss of imprinting of the insulin-like growth factor II gene in renal cell carcinoma. Cancer Res. **57:**2575–2577.
38. **Nordqvist, A. C., M. Peyrard, H. Pettersson, T. Mathiesen, V. P. Collins, J. P. Dumanski, and M. Schalling.** 1997. A high ratio of insulin-like growth factor II/insulin-like growth factor binding protein 2 messenger RNA as a marker for anaplasia in meningiomas. Cancer Res. **57:**2611–2614.
39. **Nguyen, T. T., J-C. Scimeca, C. C. Filloux, P. Peraldi, J-L. Carpentier, and E. Van Obberghen.** 1993. Co-regulation of the mitogen-activated protein kinase, extracellular signal-regulated kinase 1, and the 90-kDa ribosomal S6 kinase in PC12 cells. J. Biol. Chem. **268:**9803–9810.
40. **Okada, S., A. W. Kao, B. P. Ceresa, P. Blaikie, B. Margolis, and J. Pessin.** 1997. The 66-kDa Shc isoform is a negative regulator of the epidermal-growth factor-stimulated mitogen-activated protein kinase pathway. J. Biol. Chem. **272:**28042–28049.
41. **Okamoto, K., I. M. Morison, T. Taniguchi, and A. E. Reeve.** 1997. Epigenetic changes at the insulin-like growth factor II/H19 locus in developing kidney is an early event in Wilms tumorigenesis. Proc. Natl. Acad. Sci. USA **94:**5367–5371.
42. **Pandini, G., R. Vigneri, A. Costantino, F. Frasca, A. Ippolito, Y. Fujita-Yamaguchi, K. Siddle, I. D. Goldfine, and A. Belfiore.** Insulin/IGF-I hybrid receptors play a major role in IGF-I signaling in breast cancer. Submitted for publication.
43. **Papa, V., V. Pezzino, A. Costantino, A. Belfiore, D. Giuffrida, L. Frittitta,**

G. B. Vannelli, R. Brand, I. D. Goldfine, and R. Vigneri. 1990. Elevated insulin receptor content in human breast cancer. J. Clin. Investig. **86:**1503–1510.

44. **Parruti, G., F. Peracchia, M. Sallese, G. Ambrosini, M. Masini, D. Rotilio, and A. De Blasi.** 1993. Molecular analysis of human β-arrestin-1: cloning, tissue distribution, and regulation of expression. J. Biol. Chem. **268:**9753–9761.

45. **Roth, R. A., G. Steele-Perkins, J. Hari, C. Stover, S. Pierce, J. Turner, J. C. Edman, and W. J. Rutter.** 1988. Insulin and insulin-like growth factor receptors and responses. Cold Spring Harbor Symp. Quant. Biol. **53:**537–543.

46. **Sasaoka, T., M. Ishiki, T. Sawa, H. Ishihara, Y. Takata, T. Imamura, I. Usui, J. M. Olefsky, and M. Kobayashi.** 1996. Comparison of the insulin and insulin-like growth factor 1 mitogenic intracellular signalling pathways. Endocrinology **137:**4427–4434.

47. **Sbraccia, P., M. D'Adamo, F. Leonetti, S. Caiola, P. Iozzo, A. Giaccari, A. Buongiorno, and G. Tamburrano.** 1996. Chronic primary hyperinsulinemia is associated with altered insulin receptor mRNA splicing in muscle of patients with insulinoma. Diabetologia **39:**220–225.

48. **Sciacca, L., A. Costantino, G. Pandini, R. Mineo, F. Frasca, P. Scalia, P. Sbraccia, I. D. Goldfine, R. Vigneri, and A. Belfiore.** Insulin receptor activation by IGF-II in breast cancers: evidence for a new autocrine/paracrine mechanism. Oncogene, in press.

49. **Sell, C., M. Rubini, R. Rubin, J-P. Liu, A. Efstratiadis, and R. Baserga.** 1993. Simian virus 40 large tumor antigen is unable to transform mouse embryonic fibroblasts lacking type 1 insulin-like growth factor receptor. Proc. Natl. Acad. Sci. USA **90:**11217–11221.

50. **Shymko, M. R., P. De Meyts, and R. Thomas.** 1997. Logical analysis of timing signalling specificity: application to the insulin receptor metabolic and mitogenic signalling pathways. Biochem. J. **326:**463–469.

51. **Singer, C. F., A. Rasmussen, M. E. Lippman, and K. J. Cullen.** 1997. Coexpression of stromelysin-3 and insulin-like growth factor II in tumors of ectodermal, mesodermal, and endodermal origin: indicator of a fetal cell phenotype. J. Clin. Endocrinol. Metab. **82:**1917–1922.

52. **Soos, M. A., C. E. Field, R. Lammers, A. Ullrich, B. Zhang, R. A. Roth, A. S. Andersen, T. Kjeldsen, and K. Siddle.** 1992. A panel of monoclonal antibodies for the type I insulin-like growth factor receptor. J. Biol. Chem. **267:**12955–12963.

53. **Steele-Perkins, G., J. Turner, J. C. Edman, J. Hari, S. B. Pierce, C. Stover, W. J. Rutter, and R. A. Roth.** 1988. Expression and characterization of a functional human insulin-like growth factor I receptor. J. Biol. Chem. **263:**11486–11492.

54. **Traverse, S., N. Gomez, H. Paterson, C. Marshall, and P. Cohen.** 1992. Sustained activation of the mitogen-activated protein (MAP) kinase cascade may be required for differentiation of PC12 cells. Comparison of the effects of nerve growth factor and epidermal growth factor. Biochem. J. **288:**351–355.

55. **Ullrich, A., A. Gray, A. W. Tam, T. Yang-Feng, M. Tsubokawa, C. Collins, W. Henzel, T. Le Bon, S. Kathuria, E. Chen, S. Jacobs, U. Francke, J. Ramachandran, and Y. Fujita-Yamaguchi.** 1986. Insulin-like growth factor I receptor primary structure: comparison with insulin receptor suggests structural determinants that define functional specificity. EMBO J. **5:**2503–2512.

56. **Wang, W., P. Kumar, W. Wang, J. Epstein, L. Helman, J. V. Moore, and S. Kumar.** 1998. Insulin-like growth factor II and PAX-FKHHR cooperate in the oncogenesis of rhabdomyosarcoma. Cancer Res. **58:**4426–4433.

57. **Waters, S. B., K. H. Holt, S. E. Ross, L.-J. Syu, K.-L. Guan, A. R. Saltiel, G. A. Koretky, and J. E. Pessin.** 1995. Desensitization of Ras activation by a feedback dissociation of the SOS-Grb2 complex. J. Biol. Chem. **270:**20833–20886.

58. **Werner, H., and D. LeRoith.** 1996. The role of the insulin-like growth factor system in human cancer. Adv. Cancer Res. **68:**183–223.

59. **White, M. F.** 1997. The insulin signalling system and the IRS proteins. Diabetologia **40**(Suppl.)**:**S2–S17.

60. **Yamaguchi, Y., J. S. Flier, H. Benecke, B. J. Ransil, and D. E. Moller.** 1993. Ligand-binding properties of the two isoforms of the human insulin receptor. Endocrinology **132:**1132–1138.

61. **Zhang, L., S. Zhan, F. Navid, Q. Li, Y. H. Choi, M. Kim, P. Seth, and J. L. Helman.** 1998. AP 2 may contribute to IGF-II overexpression in rhabdomyosarcoma. Oncogene **17:**1261–1270.

62. **Zhang, L., Q. Zhan, S. Zhan, F. Kashanchi, A. J. Jr Fornace, P. Seth, and L. J. Helman.** 1998. p53 regulates human insulin-like growth factor II gene expression through active P4 promoter in rhabdomyosarcoma cells. DNA Cell Biol. **17:**125–131.